1521-009X/44/10/1697–1708$25.00
Drug Metabolism and Disposition

http://dx.doi.org/10.1124/dmd.116.072108
Drug Metab Dispos 44:1697–1708, October 2016

Utilization of Stable Isotope Labeling to Facilitate the Identification of Polar Metabolites of KAF156, an Antimalarial Agent

Su-Er W. Huskey, Ry R. Forseth, Hongmei Li, Zhigang Jian, Alexandre Catoire, Jin Zhang, Tapan Ray, Handan He, Jimmy Flarakos, and James B. Mangold

Drug Metabolism and Pharmacokinetics, Novartis Institutes for BioMedical Research, East Hanover, New Jersey

Received June 17, 2016; accepted August 1, 2016

ABSTRACT

Identification of polar metabolites of drug candidates during development is often challenging. Several prominent polar metabolites of 2-amino-1-(2-(4-fluorophenyl)-3-((4-fluorophenyl)amino)-8,8-dimethyl-5,6-dihydroimidazo[1,2-a]pyrazin-7(8H)-yl)ethanone ([^{14}C]KAF156), an antimalarial agent, were detected in rat urine from an absorption, distribution, metabolism, and excretion study but could not be characterized by liquid chromatography-tandem mass spectrometry (LC-MS/MS) because of low ionization efficiency. In such instances, a strategy often chosen by investigators is to use a radiolabeled compound with high specific activity, having an isotopic mass ratio (i.e., [^{12}C]/[^{14}C]) and mass difference that serve as the basis for a mass filter using accurate mass spectrometry. Unfortunately, [^{14}C]KAF156-1 was uniformly labeled (n = 1–6) with the mass ratio of ∼0.1. This ratio was insufficient to be useful as a mass filter despite the high specific activity (120 μCi/mg). At this stage in development, stable isotope labeled [$^{13}C_6$]KAF156-1 was available as the internal standard for the quantification of KAF156. We were thus able to design an oral dose as a mixture of [^{14}C]KAF156-1 (specific activity 3.65 μCi/mg) and [$^{13}C_6$]KAF156-1 with a mass ratio of [^{12}C]/[$^{13}C_6$] as 0.9 and the mass difference as 6.0202. By using this mass filter strategy, four polar metabolites were successfully identified in rat urine. Subsequently, using a similar dual labeling approach, [^{14}C]KAF156-2 and [$^{13}C_2$]KAF156-2 were synthesized to allow the detection of any putative polar metabolites that may have lost labeling during biotransformations using the previous [^{14}C]KAF156-1. Three polar metabolites were thereby identified and M43, a less polar metabolite, was proposed as the key intermediate metabolite leading to the formation of a total of seven polar metabolites. Overall this dual labeling approach proved practical and valuable for the identification of polar metabolites by LC-MS/MS.

Introduction

Malaria affects approximately 200 million people worldwide every year, particularly among young children in developing countries. Recent reports of drug-resistant strains to artemisinin, a first-line treatment of uncomplicated *Plasmodium falciparum* malaria, in Southeast Asia cause concerns for health authorities and the pharmaceutical industry (Haque et al., 2013; Na-Bangchang and Karbwang, 2013; Witkowski et al., 2013). Increased efforts have been undertaken to understand the mechanism of resistance toward the current artemisinin containing combination therapy (Carter et al., 2015; Hott et al., 2015).

Several antimalarial compounds are currently in phase II development and their structures are diverse, because they are either from existing or new chemical scaffolds, targeting different mechanisms of action (Held et al., 2015). Furthermore, other approaches including vaccination and next generation antimalarial drug candidates have been evaluated for efficacy and safety for malaria prophylaxis treatment (Amet et al., 2013; Sagara et al., 2014; Diagana, 2015; Nahrendorf et al., 2015; Teneza-Mora et al., 2015). Preventative treatment in children is expected to potentially avert 11 million cases and 50,000 deaths every year.

dx.doi.org/10.1124/dmd.116.072108.
This article has supplemental material available at dmd.aspetjournals.org.

KAF156 (Wu et al., 2011; Nagle et al., 2012; Fig. 1) is a first-in-class, antimalarial compound designed to eradicate both blood-stage and liver-stage malaria parasites (Meister et al., 2011; Kuhen et al., 2014; Diagana, 2015). In clinical trials, 2-amino-1-(2-(4-fluorophenyl)-3-((4-fluorophenyl)-amino)-8,8-dimethyl-5,6-dihydroimidazo[1,2-a]pyrazin-7(8H)-yl)ethanone (KAF156) has been shown to be safe and well tolerated in healthy volunteers (Leong et al., 2014). In the proof of concept trial, a single dose of KAF156 was administered to healthy volunteers either prior to or after exposure to *P. falciparum* infected mosquitoes. In both cases, KAF156 was equally effective and prevented malaria in every volunteer receiving the drug. KAF156 has the potential to be used safely for malaria prophylaxis for travelers to endemic countries, deployed soldiers, and children living in high -risk regions.

We conducted rat absorption, distribution, metabolism, and excretion (ADME) and across species in vitro metabolism studies in preparation for the above clinical investigation during the development of KAF156. Several metabolites were identified in rat plasma and feces by liquid chromatography-tandem mass spectrometry (LC-MS/MS) analysis; however, four prominent polar metabolites of KAF156, accounting for ∼24–37% of the intravenous and oral dose, were detected by radioactivity in rat urine but could not be characterized by LC-MS/MS. It was very challenging to identify these polar metabolites because of their low ionization efficiency and suspected low molecular weights.

ABBREVIATIONS: ADME, absorption, distribution, metabolism, and excretion; AUC, area under concentration-time curve; β-RAM, online radioactivity monitor; DQF-COSY, double quantum filter correlation spectroscopy; FPOAA, 2-(4-fluorophenyl)-2-oxoacetic acid; HPLC, high-performance liquid chromatography; KAF156, 2-amino-1-(2-(4-fluorophenyl)-3-((4-fluorophenyl)amino)-8,8-dimethyl-5,6-dihydroimidazo[1,2-a]pyrazin-7(8H)-yl)ethanone; LC-MS/MS, liquid chromatography-tandem mass spectrometry; MS^E, data were acquired in parallel utilizing alternating low and elevated collision energies; QC, quality control; $t_{1/2}$, the terminal elimination half-life.

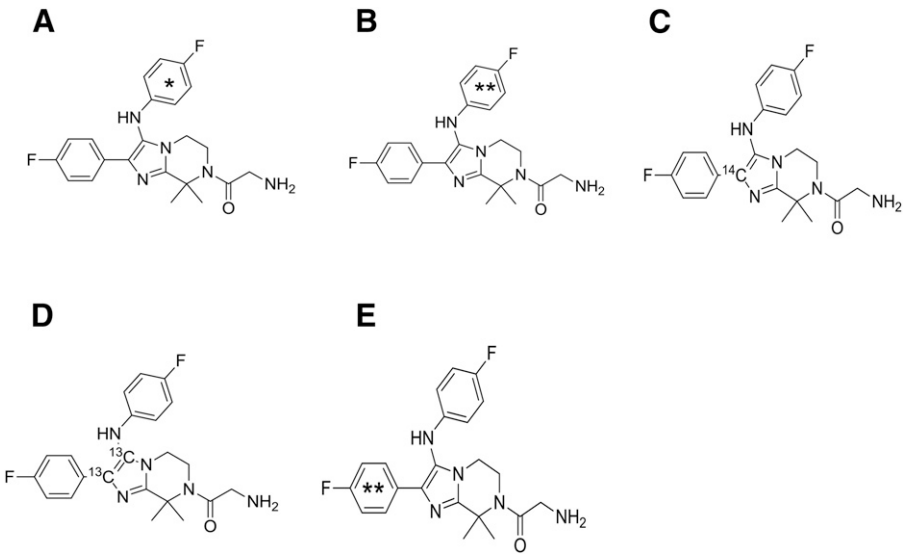

Fig. 1. Structure of (A) [^{14}C]KAF156-1, (B) [$^{13}C_6$]KAF156-1, (C) [^{14}C]KAF156-2, (D) [$^{13}C_2$]KAF156-2, and (E) [$^{13}C_6$]KAF156-3. [^{14}C]KAF156-1 was uniformly labeled with ^{14}C (n = 1-6), as indicated by *, whereas [$^{13}C_6$]KAF156-1 and [$^{13}C_6$]KAF156-3 were labeled with six ^{13}C atoms in the fluoroaniline or fluorophenyl ring, as indicated by **, respectively.

For the identification of metabolites in biologic matrices by accurate mass spectrometry, one of the strategies routinely chosen by investigators is the use of radiolabeled compound with high specific activity, where the isotopic mass ratio (e.g., [^{12}C]: [^{14}C] = 1: 0.3) is adequate to serve as a mass filter (Ma et al., 2006; Zhang and Mitra, 2012). However, the available [^{14}C]KAF156-1 (Fig. 1) was uniformly labeled (n = 1–6) with the mean ^{12}C/^{14}C mass ratio of ~0.1, which was too low to be suitable as a mass filter, although the specific activity was reasonably high (120 μCi/mg). At this stage in development, stable isotope labeled compound ([$^{13}C_6$]KAF156-1) was available for use as an internal standard for the quantification of KAF156 in toxicology studies under good laboratory practice. We took advantage of the availability of this internal standard and designed an oral dose as a mixture of [^{14}C]KAF156-1 (specific activity 3.65 μCi/mg) and [$^{13}C_6$]KAF156-1 with the mass ratio of [^{12}C]/[$^{13}C_6$] as 0.9 and mass difference of 6.0202. In principle, after dosing of [^{12}C]KAF156 and [$^{13}C_6$]KAF156-1 to rats, any metabolites containing fluoroaniline portion would be generated as isotopic pairs in vivo, sharing the signature mass ratio of 0.9 and mass difference of 6.0202, thereby rendering them easily identified using a defined mass filter by accurate mass spectrometry.

Subsequently, an alternative tracer ([^{14}C]KAF156-2) was prepared to allow detection of any putative polar metabolites that may have lost radiolabeling and were not detected using [^{14}C]KAF156-1 (Fig. 1). By using a similar dual labeling strategy, [$^{13}C_2$]KAF156-2 was synthesized and combined with [^{14}C]KAF156-2 in the oral dose to facilitate the identification of polar metabolites.

In this article, we describe the strategies and approaches used in the identification of a total of seven polar metabolites of KAF156. We also describe two unexpected hurdles we encountered during our metabolite investigations and describe solutions to overcome the challenges. Overall, the dual labeling approaches have proven to be valuable for the identification of polar metabolites with low molecular weights and low ionization efficiency.

Materials and Methods

Chemicals

KAF156 (Wu et al., 2011; Nagle et al., 2012; Fig. 1) was synthesized by Novartis Institute for Tropical Diseases [^{14}C]KAF156-1, [^{14}C]KAF156-2, [$^{13}C_6$]KAF156-1, and [$^{13}C_2$]KAF156-2 were prepared by Novartis Isotope Laboratories (East Hanover, NJ) and radiochemical purity was >99%.

4-Fluoromandelic acid, fluoroaniline, hydroxyphenylacetamide, acetonitrile, methanol, ammonium formate, and formic acid were from Sigma-Aldrich (St. Louis, MO). OPTI-FLUOR liquid scintillant was from Packard (Downers Grove, IL). Control blank plasma samples from rat were purchased from Bioreclamation (Hicksville, NY).

Animals

Male Wistar Hannover rats (~250–320 g, ~8 week, n = 24) were from Harlan Laboratories (Somerville, NJ). Catheters were surgically implanted into the carotid artery and/or jugular vein of rats by the vendor (only one catheter was implanted into carotid artery for blood collection from rats receiving oral dose). All rats were housed individually in metabolism cages (Culex Autosampler, BAS, Indianapolis, IN) in a temperature and humidity controlled room with free access to food and water (food was withheld until 4 hours postdose).

Dose Administration

All doses were administered based on the individual animal body weights on the day of dosing. As shown in Fig. 1, [^{14}C]KAF156-1 and [^{14}C]KAF156-2 with different ^{14}C labeling positions and two stable isotope labeled forms of KAF156 ([$^{13}C_6$]KAF156-1 and [$^{13}C_2$]KAF156-2) were synthesized and used for the dose preparations. A total of four subgroups of rats were dosed either intravenously or orally. For mass balance studies, [^{14}C]KAF156-1 (specific activity 66 μCi/mg at 3 mg/kg for intravenous dose and 20 μCi/mg at 10 mg/kg for oral dose) and [^{14}C]KAF156-2 (specific activity 51 μCi/mg at 3 mg/kg for intravenous dose and 21 μCi/mg at 10 mg/kg for oral dose) were dissolved in 5% Solutol HS 15 for dosing. For identification of polar metabolites, two oral doses were prepared as follows: (A) [^{14}C]KAF156-1 (specific activity 3.65 μCi/mg) and [$^{13}C_6$]KAF156-1 were combined to achieve the mass ratio [^{12}C]/[$^{13}C_6$] of 0.9 and (B) [^{14}C]KAF156-2 (specific activity 3.1 μCi/mg) and [$^{13}C_2$]KAF156-2 were combined to achieve the ratio [^{12}C]/[$^{13}C_6$] of 0.9. Both doses were prepared in 5% Solutol HS 15 for oral dosing at 10 mg/kg.

Each rat received an intravenous bolus injection via the jugular vein cannula. Oral dose was administered by gavage in rats.

Blood Collection

All rats were housed individually in Culex metabolism cages to enable automated blood sampling on the day of the study. Blood samples (200 μl) were collected from the carotid artery of rats at selected time intervals. Saline (200 μl) was automatically injected after sample was collected to clear the cannula and replace the volume of blood samples. The total blood volume collected did not exceed 1% of the body weights of rats.

Urine and Feces Collection

Urine and feces were collected daily from each of the animals for 7 days. For up to 3 days, the urine collection tubes were cooled with ice. After the final collection, each cage was rinsed with water followed by 50% methanol. The cage

wash was assayed for radioactivity. Urine and feces samples were stored at −20°C until analysis.

Sample Preparation

Plasma was obtained by centrifugation of blood samples at 4°C (2000 *g*) for 10 minutes. An aliquot of each blood sample was used for radioactivity analysis. An aliquot of plasma sample was counted directly for radioactivity. The remaining plasma samples were stored at −20°C until analysis.

Plasma for the Quantification of KAF156

Blank plasma and study samples were thawed at room temperature. Calibration standards, control blanks, and quality control (QC) samples were prepared on the day of analysis by adding appropriate standard or QC (25 μl) spiking solution to 475 μl of blank plasma. An aliquot (20 μl) of study samples, blanks, standards, or QC samples was transferred to the designated well of a 1-ml round bottom 96-well plate (Analytical Sales and Services, Pompton Plains, NJ), followed by the addition of the internal standard ([$^{13}C_6$]KAF156; 25 μl, 500 ng/ml) and acetonitrile (200 μl) for protein precipitation. Samples were mixed for 5 minutes and centrifuged at 2500 rpm for 15 minutes at 25°C. The filtrate was evaporated to dryness at ~45°C under a stream of nitrogen (TurboVap LV; Zymark Corp., Taunton, MA). The residues were reconstituted with 300 μl of acetonitrile:water: formic acid (10:90:0.1, v/v/v). An aliquot (10 μl) was analyzed for KAF156 and [$^{13}C_6$]KAF156-1 by LC-MS/MS.

Plasma for Metabolic Profiling of KAF156

All plasma samples were thawed at room temperature and aliquots (150 μl) were pooled from each animal at each time point. Each pool was diluted with 250 μl water and extracted with 2 ml of acetonitrile:methanol:acetic acid (50:50: 0.1, v/v/v). The samples were vortex-mixed followed by centrifugation. The supernatants were evaporated to near dryness under a stream of nitrogen. The residues were reconstituted with 100 μl of acentonitrile:deionized water (50:50; v/v) and an aliquot was analyzed by LC-MS/MS.

Urine for Metabolic Profiling of [^{14}C]KAF156-1 and [^{14}C]KAF156-2

Urine pools (10–20% by volume) were prepared with samples collected from rats during 0–24 or 0–72 hours postdose. The selected time interval represented >91–95% of the total urinary excretion of radioactivity from rats by either dosing route. The pooled samples were centrifuged at 3500 rpm for 10 minutes, and aliquots of the resulting supernatant were analyzed by LC-MS/MS.

Feces for Metabolic Profiling of [^{14}C]KAF156-1 and [^{14}C]KAF156-2

Rat feces were collected in 24-hour intervals for 7 days. Fecal samples from each rat from each collection interval were homogenized with 2 × water separately. Fecal homogenates, representing ~5–10% of total weight, were pooled from three rats and from 0- to 24-hour and 24- to 48-hour intervals. The selected time interval represented >93% of the total radioactivity excreted in rat

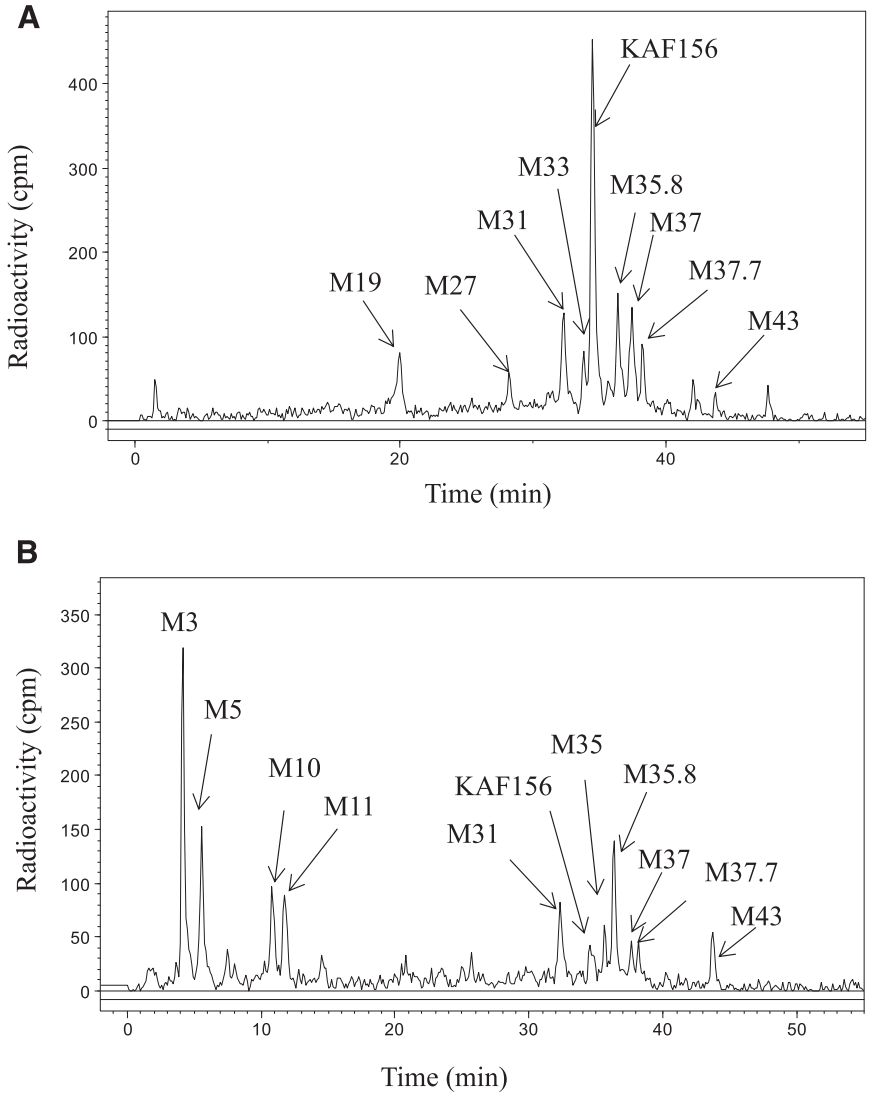

Fig. 2. Representative metabolic profiles in (A) pooled fecal extracts and (B) pooled urine after oral dosing of [^{14}C]KAF156-1 to rats. Urine and feces samples were collected daily from rats up to 7 days. After homogenization, fecal homogenates were pooled, extracted, and analyzed by LC-MS/MS. The HPLC separation of KAF156 and metabolites was performed, as described in *Materials and Methods* (method A).

feces by either intravenous or oral dosing route. The resulting fecal pools were extracted three times with three volumes of acetonitrile:methanol:acetic acid (50:50:0.1, v/v/v). After centrifugation at 3500 rpm for 10 minutes, the supernatants were combined and concentrated under a stream of nitrogen. Residues were reconstituted with acetonitrile:deionized water (50/50, v/v) and analyzed by LC-MS/MS. The excretion recoveries of radioactivity from rat feces were ~68–78% (i.v.) and ~69–77% (oral), respectively.

Sample Analysis

Determination of Radioactivity. The radioactivity of all samples was determined by liquid scintillation counting. For quench correction, an external standard ratio method was used. Quench correction curves were established by means of sealed standards. An aliquot of plasma, urine samples, and cage wash was counted directly for radioactivity.

Solvable (500 μl) was added to each blood sample and incubated in a shaking water bath at 50°C for 2 hours. After incubation, 50 μl of 100 mM EDTA as an antifoaming agent and 200 μl of 30% hydrogen peroxide were added to decolorize the samples. The sample vials were loosely capped and returned to the water bath for 3 hours. Thereafter, 10 ml of Eq. 989 scintillation cocktail was added and the samples were placed in the dark overnight to reduce chemiluminescence before counting for radioactivity.

Fecal samples from animals were homogenized with two or three volumes of water. Duplicate samples (~100 mg) of the slurry were weighed into scintillation vials and processed as described above for blood samples before radioactivity determination. The remaining fecal homogenate was stored frozen at −20°C until LC-MS/MS analysis.

Quantification of KAF156 by LC-MS/MS

Samples were analyzed on an LC-MS/MS system consisting of a Shimadzu HPLC System and Sciex API5000 mass spectrometer using Analyst software version 1.4.2 (Foster City, CA). The mass spectrometer was operated in the positive ion mode, using turbo spray ionization, with a source temperature of 500°C. Chromatographic separation was carried out on a Zorbax SB-C8 50 × 4.6 mm column at 40°C. KAF156 and the internal standard ([$^{13}C_6$]KAF156-1, Fig. 1) were eluted using a gradient method with a mobile phase consisting of (A) 10 mM ammonium acetate in water containing 0.03% trifluoracetic acid and (B) 10 mM ammonium acetate in methanol containing 0.03% trifluoracetic acid. The gradient was 30%B for 0.01 minute increased to 95%B from 0.01 to 1 minute; followed by a 1.2-minute hold at 95%B. The flow rate was 0.6 ml/min. The multiple reaction monitoring transitions for KAF156 and [$^{13}C_6$]KAF156-1 were *m/z* 412.4 to *m/z* 312.1 and *m/z* 418.5 to *m/z* 318.1, respectively.

Calibration curves were generated by plotting the respective peak area ratios (y) of KAF156 to the internal standard versus the concentrations (x) of the calibration standards using weighted $1/x^2$ quadratic least-squares regression. The quantification was performed using Analyst software and Watson LIMS version 7.2.0.01. Concentrations in QC and study samples were calculated from the resulting peak area ratios and interpolation from the regression equations of the calibration curves. The lower limit of quantification was 1.0 ng/ml.

Metabolic Profiling by LC-MS/MS

Metabolic profiling was performed on a Waters Acquity UPLC System (Waters Corp., Milford, MA) equipped with an autosampler and a quaternary pump and an online radioactivity monitor (β-RAM) or a fraction collector. Two UPLC methods were developed for the separation of KAF156 and metabolites.

Method A: The separation of metabolites was carried out on a Zorbax SB-C18 column (150 × 3.0 mm, 3.5 μm) using a linear gradient with a mobile phase consisting of (A) 5 mM ammonium formate containing 0.1% formic acid and (B) acetonitrile containing 0.1% formic acid. The gradient was 2%B for 3 minutes; increased to 25%B from 3 to 32 minutes; increased to 60%B from 32 to 45 minutes; increased to 95%B from 45 to 52 minutes; hold at 95%B from 52 to 60 minutes. The flow rate was 0.7 ml/min.

Method B: The separation of polar metabolites was carried out on a UPLC HSS T3 column (150 × 3.0 mm, 1.8 μm) using a linear gradient with a mobile phase consisting of (A) 5 mM ammonium formate containing 0.1% formic acid; and (B) acetonitrile containing 0.1% formic acid. The gradient was 2%B for 8 minutes; increased to 25%B from 8 to 18 minutes; increased to 60%B from 18 to 34 minutes; increased to 95%B from 34 to 38 minutes; hold at 95%B from 38 to 40 minutes. The flow rate was 0.5 ml/min.

The HPLC column eluent was split 1:4 (MS/fraction collector or MS/β-RAM). The eluent from the fraction collector was mixed with methanol (0.5 ml/min) and collected directly into 96-Deepwell LumaPlates (Perkin Elmer, Downers Grove, IL) coated with solid scintillant at 0.15 minutes/well using a fraction collector. The plates were dried at 40°C under a stream of nitrogen. The plates were counted for 10–15 minutes/well in a TopCount Model NXT radioactivity detector (Perkin-Elmer Life Sciences, Waltham, MA). Online monitoring with β-RAM employed a 250 μl liquid cell, and eluent was mixed with 1.4 ml/min IN-Flow 2:1 (IN/US Systems, Tampa, FL) liquid scintillant. The resulting data were processed using the Laura Data System (LabLogic, Inc., ver. 4.0, Brandon, FL). All quantification was based on the radioactivity associated with the radiochromatographic peaks.

LC-MS Instrumentation and Operating Conditions

The structural characterization of metabolites was carried out using the above UPLC method coupled to a two-channel Z-spray (LockSpray) Waters Synapt G1 or G2 quadrupole time-of-flight mass spectrometer (Manchester, UK). The Q-TOF Synapt was operated in V-mode with a typical resolving power of at least 10,000. Qualitative analyses were carried out using electrospray ionization in the positive or negative ion mode using a lock spray source. Leucine enkephalin was used as the mass reference standard for exact mass measurements and was delivered via the second spray channel at a flow rate of 5–10 μl/min.

Accurate mass LC/MS data were collected using MS^E approach where data were acquired in parallel utilizing alternating low and elevated collision energies. In low-energy MS mode, data were collected at consistent collision energy of 12 eV. In elevated MS^E mode, collision energy was ramped from 15 to 30 eV during data collection cycle.

Metabolites were characterized by TOF MS full scan and product ion scans. Product ion scans were obtained either from dedicated TOF MS/MS experiments or the MS^E approach. With TOF MS/MS experiments, the trapping collision energy was ramped from 15 to 20 eV, whereas the transferred collision energy was set at 6 eV. In the MS^E approach, the data were acquired in parallel using alternating low and elevated collision energies. Argon was used as the collision gas for both product ion scanning techniques. Acquiring data with the MS^E approach provided for collection of intact precursor ions and fragment ion information.

NMR Analyses of Polar Metabolites (M7, M10.1, and M12)

Detailed description for the synthesis of 2-(4-fluorophenyl)-2-oxoacetic acid (M7) and the isolation of polar metabolites from rat urine can be found in

TABLE 1

Fragmentation patterns of KAF156 and metabolites under positive ion mode

Structural characterization of metabolites was carried out by LC-MS/MS analysis with accurate mass measurements. The proposed structures of the metabolites were based on their elemental composition derived from accurate mass measurements and fragment ions in their data dependent MS^2 and MS^3 mass spectra. Comparison of metabolite fragment ions with those of KAF156 allowed the assignment of regions of biotransformation.

Compound	[MH^+] *m/z*	Elemental Formula	Diagnostic Fragment Ions[a]
KAF156	412.1959	$C_{22}H_{24}N_5OF_2$	412, **312**, 245, 124, 101, 72
M19	410.2000	$C_{22}H_{25}N_5O_2F$	410, **310**, 243,122, 101
M24	431.1909	$C_{22}H_{25}N_4O_3F_2$	**431**, 413, 373, 231
M27	452.2107	$C_{24}H_{27}N_5O_3F$	452, **310**, 243, 143, 101
M28	411.1844	$C_{22}H_{24}N_4O_3F$	411, **310**, 243, 200, 102
M31	428.1898	$C_{22}H_{24}N_5O_2F_2$	428, 410, 371, 312, **307**, 207, 168, **123**, 111, 95, 70
M33	383.1693	$C_{21}H_{21}N_4OF_2$	383, 355, 339, **312**, 245, 124, 122
M35	444.1847	$C_{22}H_{24}N_5O_3F_2$	444, 426, 383, 369, **329**, 312, 290, 286, 245, 193, 141, 123, 98, 70
M35.8	428.1890	$C_{22}H_{24}N_5O_2F_2$	428, 410, 371, **331**, 314, **288**, 245, **220**, 177, **141**, 124, 98, 70
M36	454.2061	$C_{24}H_{26}N_5O_2F_2$	454, **312**, 245, 143, 101
M37	429.1720	$C_{22}H_{23}N_4O_3F_2$	429, **383**, 355, **312**, 272, 245, 124, 84
M37.7	413.1794	$C_{22}H_{23}N_4O_2F_2$	413, **312**, 245, 124, 102

[a]The most abundant fragment ions are highlighted in bold.

TABLE 2

Fragmentation patterns of KAF156 and metabolites under negative ion mode

Structural characterization of metabolites was carried out by LC-MS/MS analysis with accurate mass measurements. The proposed structures of the metabolites were based on their elemental composition derived from accurate mass measurements and fragment ions in their data dependent MS^2 and MS^3 mass spectra. Comparison of metabolite fragment ions with those of KAF156 allowed the assignment of regions of biotransformation.

Compound	[MH-] m/z	Elemental Formula	Diagnostic Fragment Ions[a]
KAF156	410.1792	$C_{22}H_{22}N_5OF_2$	410, 335, **310**
M3	205.9927	$C_6H_5NO_4FS$	**206**, 188, **126**, 106
M5	230.0126	$C_8H_8NO_5S$	**230**, 213, **150**, **107, 97**
M7	167.0145	$C_8H_4FO_3$	167, 139, **95**, 75
M10	168.0468	$C_8H_7NO_2F$	168, **126**, 106
M10.1	169.0309	$C_8H_6FO_3$	**169**, **125**, 95
M11	248.0030	$C_8H_7NO_5FS$	**248**, **168**, **126**, 97
M12	196.0416	$C_9H_7FNO_3$	**196**, **153**, 95
M43	260.0525	$C_{14}H_8NO_2F_2$	**260**, 232, **206**, 166, 149, 136, 116, 110, 95

[a]The most abundant fragment ions are highlighted in bold.

Supplemental Materials. ^1H spectra were acquired for enriched M7, M10.1, and M12 from urine samples as well as two reference compounds [4-fluoromandelic acid and 2-(4-fluorophenyl)-2-oxoacetic acid; ~100 μg]. All samples were dissolved in acetonitrile-d_3.

NMR spectra were acquired on a Bruker UltraShield 600 MHz/54 mm spectrometer equipped with a 5 mm CP TXI 600S3 H-C/N-D-05 Z Cryoprobe. For the double quantum filter correlation spectroscopy (DQF-COSY) spectrum, the 90° pulse (P1) was calibrated at a ^1H transmitter power of 0.2 dB, and the following acquisition parameters were used: acquisition time = 0.75 second, complex increments = 1024, and number of scans = 32. Spectra were processed in MestReNova. DQF-COSY spectra were processed using 8k (f2) by 2k (f1) zero filling. A sine squared window function was applied in both the t1 and t2 dimensions. Detailed description for the NMR analyses of three polar metabolites from rat urine can be found in Supplemental Materials.

Data Processing

Quantification of KAF156 and Metabolites by Radiometry. KAF156 and metabolites were quantified in the extracts by radiochromatography. Peaks were selected visually from the radiochromatogram, and their corresponding areas were determined via peak integration (LAURA).

The percent of radioactivity (PRA) in a particular peak, Z, was calculated as following:

$$\%\ \text{PRA in Z} = \frac{\text{DPM in peak Z}}{\text{total DPM in all integrated peaks}} \times 100$$

The concentration or amount of each component was calculated as %PRA (as a fraction) multiplied by the total concentration (ngEq/ml) or percent of dose in the excreta.

Pharmacokinetic Parameters

The pharmacokinetic parameters were calculated using actual recorded sampling times and noncompartmental method(s) with Phoenix (WinNonlin Version 6.2, Pharsight, Certara L.P. Princeton, NJ). Concentrations below the lower limit of quantification were treated as zero for pharmakokinetic parameter calculations. The linear trapezoidal rule was used for AUC calculation. Regression analysis of the terminal plasma elimination phase for the determination of $t_{1/2}$ included at least three data points after C_{max}. If the adjusted R^2 value of the regression analysis of the terminal phase was less than 0.75, no values were reported for $t_{1/2}$, AUC_{inf}, V_z/F, and CL/F.

Results

Mass Balance and Pharmacokinetics of KAF156 in Rats

After intravenous or oral dosing of [^{14}C]KAF156-1 or [^{14}C]KAF156-2 (Fig. 1), mass balance was achieved in rats, with 93–118% of the administered radioactivity dose being recovered in excreta. Higher than

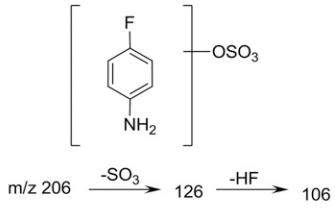

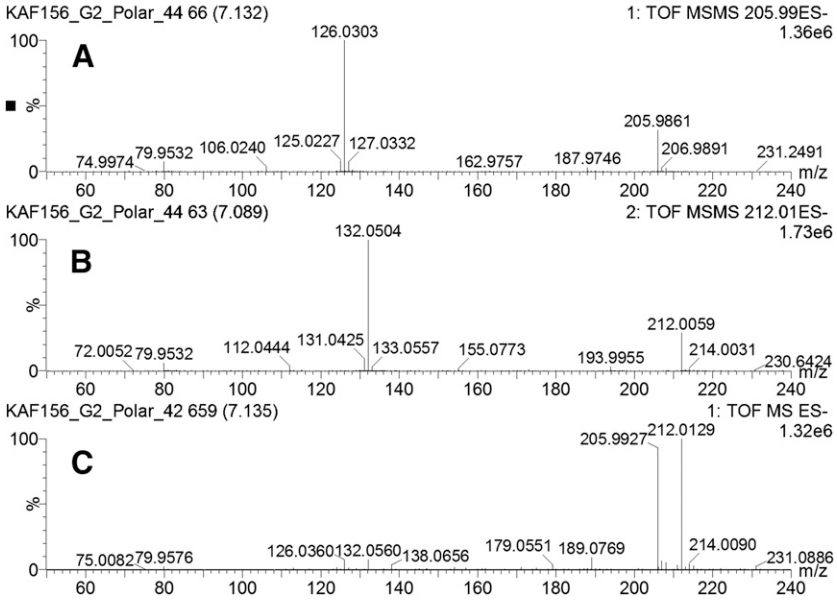

Fig. 3. Negative product ion spectra of M3 from urine after oral dosing of [^{14}C]KAF156-1 and [$^{13}C_6$]KAF156-1 to rats. The oral dose consisted of [^{12}C]KAF156, trace amount of [^{14}C]KAF156-1 and [$^{13}C_6$]KAF156-1. The mass ratio of 0.9 and mass difference of 6.0202 Da was used as mass filters for the detection of ^{12}C and $^{13}C_6$ molecular ions [e.g., 205.9927 and 212.0129 in (C)]. As expected, product ion spectra of M3 showed pairs of fragments with mass difference of 6.0202 Da [e.g., 126.0303 and 132.0504 in (A and B)].

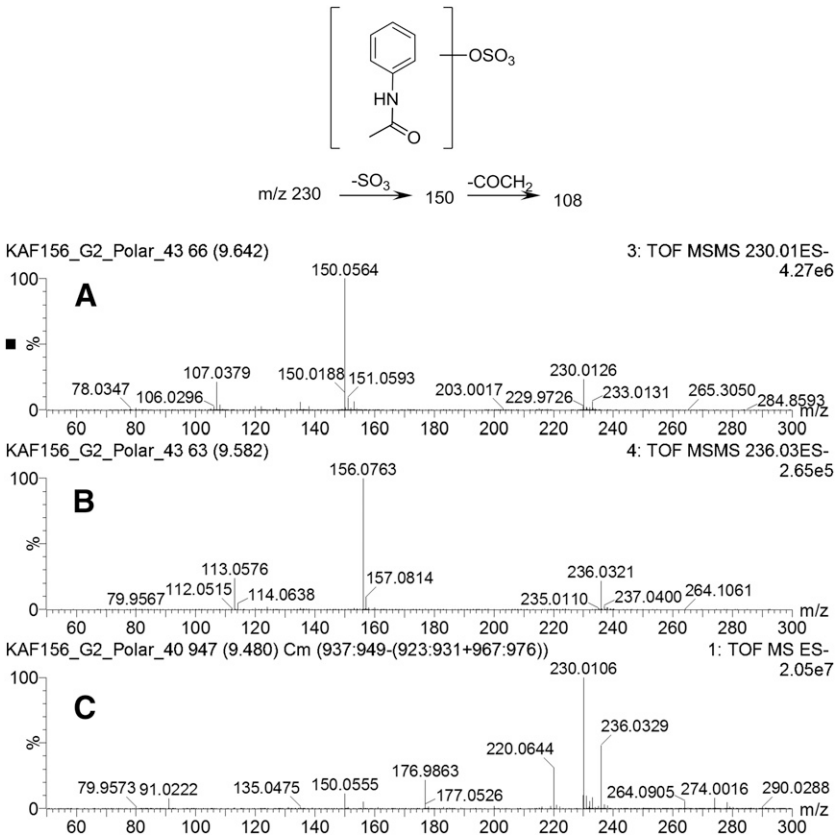

Fig. 4. Negative product ion spectra of M5 from urine after oral dosing of [^{14}C]KAF156-1 and [$^{13}C_6$]KAF156-1 to rats. The oral dose consisted of [^{12}C]KAF156, trace amount of [^{14}C]KAF156-1 and [$^{13}C_6$]KAF156-1. As expected, full and product ion spectra of M5 showed isotopic pairs of molecular ions (C) and corresponding fragment ions (A and B) with mass ratio of 0.9 and mass difference of 6.0202 Da.

100% of radioactivity recovered in excreta was considered within experimental errors (e.g., pipetting, weighing, and counting, etc.). Two tracers ([^{14}C]KAF156-1 and [^{14}C]KAF156-2 with different ^{14}C labeling positions) were used in mass balance studies. After intravenous or oral dosing of [^{14}C]KAF156-1, excretion of radioactivity was about equal (~40–56% in urine and ~61–63% in feces). However, after intravenous or oral dosing of [^{14}C]KAF156-2, radioactivity was primarily excreted into feces (~23% in urine and ~68–75% in feces).

After intravenous dosing, KAF156 had a moderate terminal half-life ($t_{1/2}$; 6.6 hours), high plasma clearance (CL; 5.4 l/h/kg) and large volume of distribution at steady state (V_{ss}; 29.5 l/kg). After oral doing, KAF156 absorption rate was moderate with C_{max} of 139 ng/ml observed at 2 hours (time to reach the maximum concentration after drug administration). The extent of oral absorption was at least 55%, based on the ratio of the dose-normalized total radioactivity AUC for plasma obtained from orally versus intravenously dosed rats (data not shown). The estimated oral bioavailability was ~48%, indicating minimal

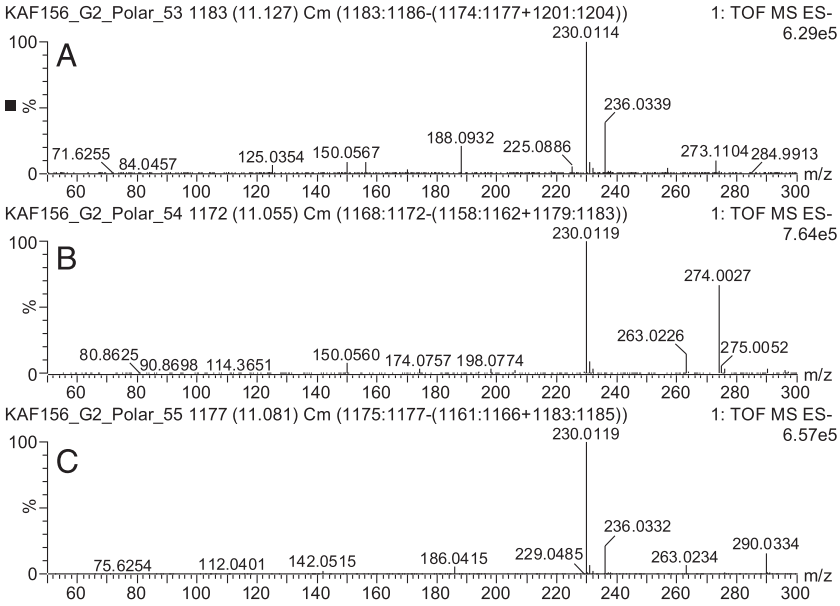

Fig. 5. Negative product ion spectra of M5 (A) urine from rats dosed orally with [^{14}C]KAF156-1 and [$^{13}C_6$]KAF156-1, (B) urine from control rats, and (C) mixture of urine from (A) and (B). LC-MS/MS analysis was performed from (A) urine samples from rats orally dosed with [^{14}C]KAF156-1 and [$^{13}C_6$]KAF156-1 and (B) urine collected from control rats where molecular ion of *m/z* at 230 was detected. [M-H]$^-$ of *m/z* at 230 was detected with identical UPLC elution time when above two samples were mixed together.

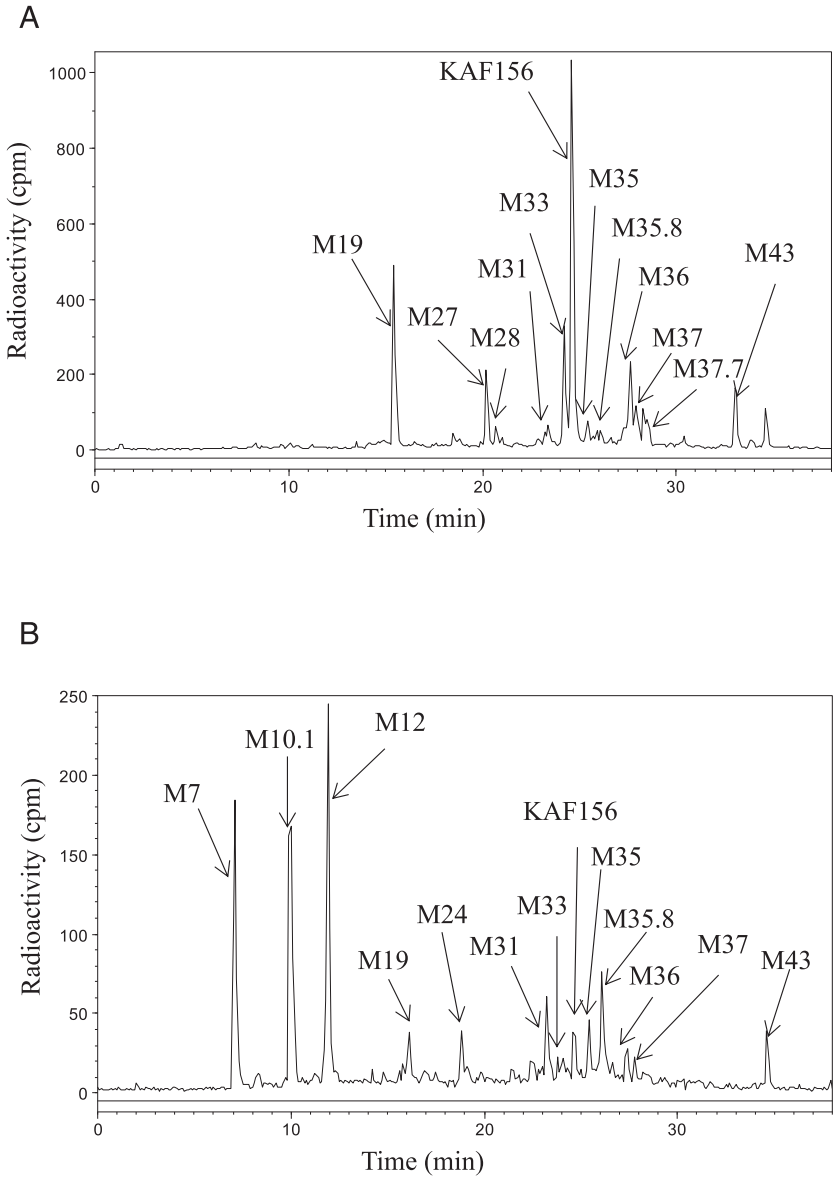

Fig. 6. Representative metabolic profiles in (A) pooled fecal extracts and (B) pooled urine after oral dosing of [^{14}C]KAF156-2 to rats. Urine and feces samples were collected daily from rats up to 7 days. After homogenization, fecal homogenate were extracted and analyzed by LC-MS/MS. The HPLC separation of KAF156 and metabolites was performed, as described in *Materials and Methods*.

first-pass effect in rats. Detailed summary tables of mass balance and pharmakokinetic parameters can be found in the Supplemental Tables S1 and S2.

Metabolite Profiling of [^{14}C]KAF156-1 or [^{14}C]KAF156-2 in Rat Plasma

After intravenous dosing of [^{14}C]KAF156-1 or [^{14}C]KAF156-2, the prominent radiolabeled components in plasma were KAF156 and three oxidative metabolites (M31, M35.8, and M37), each accounting for ~12–35% of the total radioactivity $AUC_{0\text{-}8\ hours}$. Nomenclature of metabolites was based on their HPLC elution time in the study in which they were first identified. Detailed graphic presentation can be found in the Supplemental Figs. S1 and S2.

Metabolite Profiling of [^{14}C]KAF156-1 in Rat Feces

KAF156 was well absorbed and extensively metabolized in rats such that unchanged KAF156 in feces accounted for ~8–21% of the dose by either intravenous or oral dosing route (Fig. 2A). Several minor metabolites (M19, M27, M31, M33, M35, M35.8, M37, M37.7, and M43) were identified in rat feces, each accounting for ~2–10% of the dose by either dosing route.

Characterization of Metabolites of [^{14}C]KAF156-1 in Rat Feces

The structures of the metabolites were proposed based on their elemental composition derived from accurate mass measurements (<3–5 ppm), fragment ions in their data-dependent MS^2 and MS^3 mass spectra. Elemental formula and diagnostic fragmentation ions of KAF156 and metabolites are summarized in Tables 1 and 2.

KAF156 ($[MH]^+$ = 412) produced fragments at *m/z* 312 (loss of ethyl amino acetamide), 245 (loss of HCN from fluorophenyl imidazole amine), 101 (ethyl amino acetamide), and 124 (fluoro-benzylideneamine) when analyzed in positive ion mode. Detailed product ion spectra of KAF156 can be found in Supplemental Fig. S3.

Metabolite Profiling of [^{14}C]KAF156-1 in Rat Urine

A representative radiochromatogram shows the metabolic profiles in urine after an oral dose of [^{14}C]KAF156-1 to rats (Fig. 2B). KAF156 and six minor metabolites (M31, M35, M35.8, M37, M37.7, and M43) were

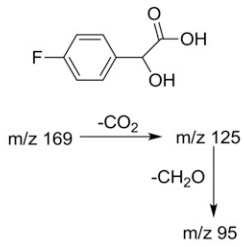

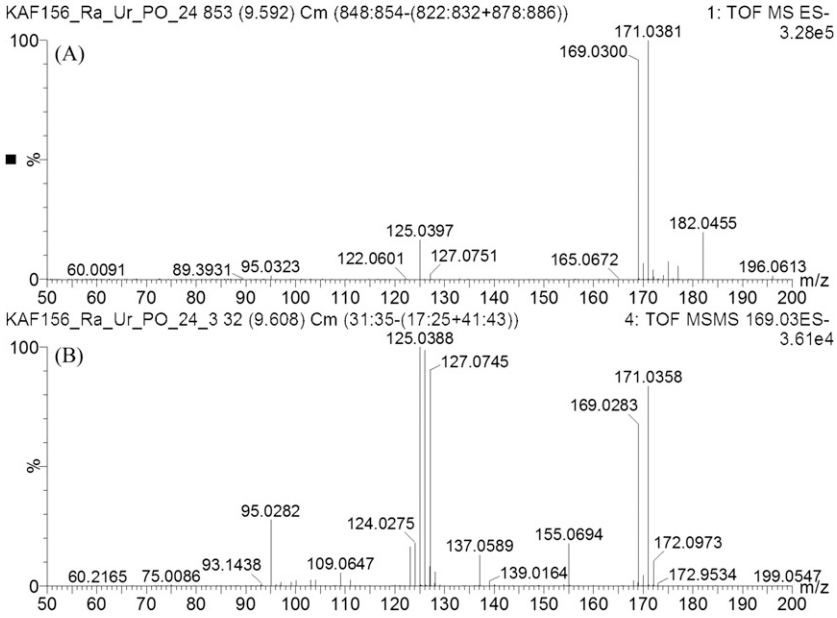

Fig. 7. Negative product ion spectra of M10.1 from urine after oral dosing of [^{14}C]KAF156-2 and [$^{13}C_2$]KAF156-2 to rats. The oral dose consisted of [^{12}C]KAF156, trace amount of [^{14}C]KAF156-2 and [$^{13}C_2$]KAF156-2. The mass response ratio of 0.9 and mass difference of 2.0060 Da were used as mass filters for the detection of ^{12}C and $^{13}C_2$ molecular ions [e.g., 169.0300 and 171.0381 at (A)]. As expected, product ion spectra of M10.1 showed pairs of fragments with mass difference of 2.0060 Da [e.g., 125.0388 and 127.0745 at (B)].

identified in rat urine. Additionally, four relatively polar metabolites (M3, M5, M10, and M11) were detected by radiochromatography, together accounting for ~35% of the intravenous dose and ~23% of the oral dose. Their structures were not identified because of their poor ionization efficiency under either positive or negative ion mode, their suspected low molecular weights, their relatively short UPLC elution times (~3–11 minutes), and endogenous urine matrix background. A new UPLC method was developed to extend the UPLC elution times of the polar metabolites (~7–18 minutes), as described as method B in *Materials and Methods* (graphic presentation can be found in Supplemental Fig. S4).

Characterization of Polar Metabolites of [^{14}C]KAF156-1 in Rat Urine

To facilitate the identification of polar metabolites, a mixture of [^{14}C]KAF156-1 (specific activity 3.65 μCi/mg) and [$^{13}C_6$]KAF156-1 was dosed orally to rats. By using the dual labeling approach, three polar metabolites (M3, M10, and M11) were identified by LC-MS/MS analysis using defined mass filters and analyzed under negative ion mode.

As shown in Fig. 3A, M3 ($[M-H]^-$ = 206) was assigned as a *O*-sulfonate conjugate of hydroxylated fluoroaniline. The product ion spectrum showed the characteristic fragments *m/z* 126 (loss of SO_3) and 106 (loss of HF from *m/z* 126). As expected, [$^{13}C_6$]M3 ($[M-H]^-$ = 212, ^{13}C isotope ion) generated corresponding fragments at *m/z* 132 and 112 (Fig. 3B). By using the same isotopic filtering approach, two polar metabolites (M10 and M11) and one less polar metabolite (M43) were identified and their fragment ions are summarized in Tables 1 and 2. Detailed product ion spectra of M43 can be found in Supplemental Fig. S5.

However, M5 remained unidentified when the mass filters were set at isotopic mass ratio of 0.9 and mass difference at 6.0202 Da. Only when the isotopic mass ratio of 0.9 was removed from the mass filter, was M5 ($[M-H]^-$ = 230) detected with mass difference at 6.0202 Da. M5 was assigned to be a *O*-sulfonate conjugate of acetylated and hydroxylated aniline. Interestingly, M5 has lost fluorine versus other polar metabolites (M3, M10, and M11). Presumably, oxidative defluorination at fluoroaniline has occurred to form M5. The product ion spectrum showed fragments at *m/z* 150 (loss of SO_3) and 107 (loss of acetyl group from *m/z* 150) (Fig. 4A). Similarly, [$^{13}C_6$]M5 ($[M-H]^-$ = 236, ^{13}C isotope ion) generated corresponding fragments at *m/z* 156 and 113 (Fig. 4B).

As shown in Fig. 4C, the ratio of [^{12}C]/[$^{13}C_6$] changed from 0.9 to ~2, indicating that this metabolite had lost fluorine and coeluted with an endogenous substance with the same molecular ion of *m/z* at 230. Indeed, an endogenous substance with $[M-H]^-$ at *m/z* 230 was detected in urine from untreated rat (Fig. 5B), which coeluted with M5 in the UPLC system used in the study (Fig. 5C).

Metabolite Profiling of [^{14}C]KAF156-2 in Rat Feces

To identify any putative metabolite that had lost radiolabeling using [^{14}C]KAF156-1, another tracer, [^{14}C]KAF156-2 (Fig. 1), was synthesized for an additional rat ADME study. Consistent with findings from [^{14}C]KAF156-1, KAF156 was well absorbed and extensively metabolized in rats such that unchanged KAF156 in feces accounted for ~8–25% of the dose by either intravenous and oral dosing route (Fig. 6A). Several metabolites (M19, M27, M33, M36, and M43) were identified in rat feces, each accounting for ~5–13% of the intravenous or oral dose. Several minor metabolites (M28, M31, M35, M35.8, M37, M37.7), each

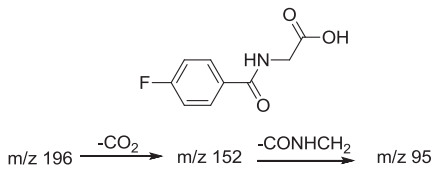

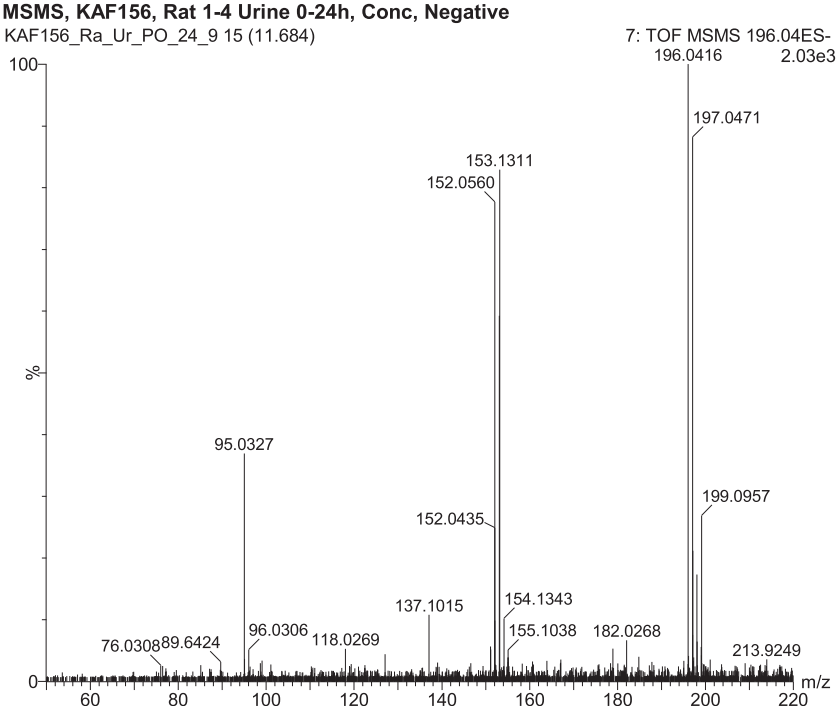

Fig. 8. Negative product ion spectra of M12 from urine after oral dosing of [^{14}C]KAF156-2 and [$^{13}C_2$]KAF156-2 to rats. The oral dose consisted of [^{12}C]KAF156, trace amount of [^{14}C]KAF156-2 and [$^{13}C_2$]KAF156-2. The mass difference of 2.0060 Da was lost, presumably M12 had lost one ^{13}C during biotransformation. Two companion molecular ions (e.g., 196.0416 versus 197.0471) were detected and product ion spectra showed pairs of fragment ions (152.0560 versus 153.1311).

accounting for <3% of the intravenous or oral dose, were identified in rat feces. Elemental formula and diagnostic fragmentation ions of KAF156 and metabolites are summarized in Tables 1 and 2.

Metabolite Profiling of [^{14}C]KAF156-2 in Rat Urine

A representative radiochromatogram shows the metabolic profiles in urine after an oral dose of KAF156 to rats (Fig. 6B). KAF156 and several minor metabolites (M19, M24, M31, M33, M35, M35.8, M36, M37, and M43) were identified in rat urine. However, three relatively polar metabolites (M7, M10.1, and M12), accounting for ~13–14% of the dose by either intravenous or oral dosing route, remained unidentified because of their low ionization efficiency under positive or negative ion mode and substantial urine matrix background. Four previously identified polar metabolites (M3, M5, M10, and M11) were detected by LC-MS/MS and the absence of the ^{14}C radiolabel in these chemical species precluded their quantification via radiochromatography in this study.

Characterization of Polar Metabolites of [^{14}C]KAF156-2 in Rat Urine

By using the same dual labeling approach, a mixture of [^{14}C]KAF156-2 (specific activity 3.1 μCi/mg) and [$^{13}C_2$]KAF156-2 with the ratio of [^{12}C]/[$^{13}C_2$] as 0.9 was dosed orally to rats. By using the isotope mass ratio of 0.9 and the mass difference of 2.006 Da as mass filters, two polar metabolites (M7 and M10.1) were identified using LC-MS/MS analysis under negative ion mode.

As shown in Fig. 7, the metabolite M10.1 ([M-H]$^-$ = 169) was assigned as 4-fluoromandelic acid. The product ion spectrum showed characteristic fragments *m/z* 125 (loss of CO_2) and 95 (loss of CH_2O from *m/z* 125). As expected, [$^{13}C_2$]M10.1 ([M-H]$^-$ = 171, ^{13}C isotope ion) generated corresponding fragments at *m/z* 127 and 95. Apparently, the fragment ion at *m/z* 95 was the same for both [^{12}C] and [$^{13}C_2$] molecules because the fragment ion of *m/z* at 95 excluded two stable isotope labeled carbon atoms. By using the same approach, M7 was identified as the corresponding fluorophenyl oxoacetic acid. The fragment ions of these polar metabolites are summarized in Tables 1 and 2.

However, the metabolite M12 remained unidentified when the mass filters were set at isotope mass ratio of 0.9 and mass difference at 2.002 Da. Presumably one of the two stable isotope labeled carbon atoms was lost during biotransformation, and the mass difference was no longer 2.002 Da (see below NMR analysis and Fig. 8).

Structural Elucidation of Polar Metabolites by NMR

4-Fluoromandelic acid was purchased from Sigma Aldrich and 2-(4-fluorophenyl)-2-oxoacetic acid was synthesized according to the published procedure (Lee and Chen, 1991). The metabolites M7, M10.1, and M12 were isolated from rat urine, and their structures were explored using NMR analyses via comparison with the two reference compounds of 4-fluoromandelic acid and 2-(4-fluorophenyl)-2-oxoacetic acid (FPOAA).

DQF-COSY spectra acquired for the enriched M7-containing urine samples were compared with authentic FPOAA. Additionally, DQF-COSY spectra for the enriched M10.1-containing urine samples were compared with the 4-fluoromandelic acid standard. For both M7 and M10.1, the spectral data matched their corresponding authentic standards as assessed by comparison of chemical shifts and coupling patterns. These NMR data supported the proposed structures based on the initial mass spectrometric analysis of the polar metabolites M7 and M10.1.

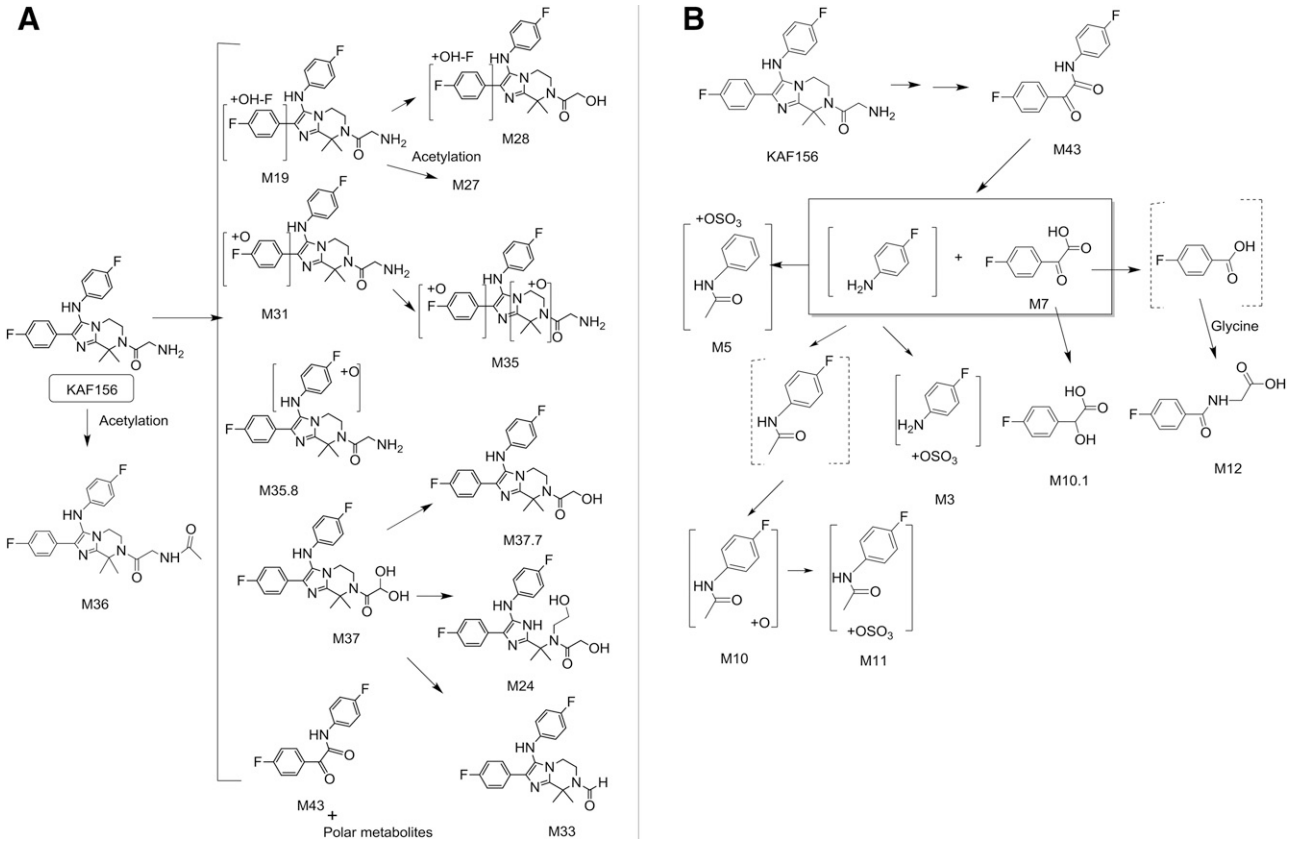

Fig. 9. Proposed metabolic pathways of KAF156 in rats (A) less polar metabolites and (B) polar metabolites. Structures of metabolites were characterized by LC-MS/MS analyses. Positive ion mode was used for the identification of less polar metabolites whereas negative ion mode was used for the identification of polar metabolites except negative ion mode was used for the identification of a less polar metabolite M43. Proposed structures of M7, M10.1, and M12 were further confirmed by NMR analyses.

The ^{1}H spectrum acquired for the M12-enriched NMR sample showed two peaks shifted downfield that integrate with whole-number ratios relative to each other (7.93 and 8.66 ppm; relative integration, 2:1). The chemical shift and relative integration of the signal at 8.66 ppm suggested that this peak represents an amide proton. A DQF-COSY spectrum acquired for the sample revealed that the putative amide proton couples to a methylene at 3.82 ppm. Additionally, the DQF-COSY coupling patterns observed for the aromatic protons at 7.93 ppm were indicative of an aryl group with a fluorine atom substituted at the para position. Further structural analysis via the acquisition of a rotational frame nuclear Overhauser effect spectroscopy spectrum demonstrated that the amide proton is proximal to the aromatic protons observed at 7.93 ppm. The chemical shift and position of the methylene, distal to the aromatic ring, was consistent with it being positioned between the amide nitrogen and a carboxylic acid group. This conclusion was supported by mass spectrometric analysis (Fig. 8) and comparison of observed NMR chemical shifts to those reported for 4-fluoro-hippuric acid (Chavez et al., 2010).

Detailed description of the FPOAA synthesis and NMR analyses can be found in the Supplemental Materials and Supplemental Figs. S6–S13.

In Vitro Metabolism of KAF156 in Rat and Human Hepatocytes

[^{14}C]KAF156-1 (2.5 and 12.5 μM) was incubated in freshly prepared hepatocyte suspensions for 24 hours. The prominent metabolites were M37.7, M19, M27, and M43 in rat hepatocytes; M36, M37.7, and M43 in human hepatocytes, respectively. However, no polar metabolites were generated from hepatocytes, although M43 was a prominent metabolite in vitro (graphic presentation can be found in Supplemental Fig. S14).

Proposed Metabolite Pathways of [^{14}C]KAF156 in Rats

Metabolic pathways of KAF156 in rats are summarized in Fig. 9. KAF156 was well absorbed and extensively metabolized in rat and unchanged KAF156 only accounted for ~8–25% of the dose by either dosing route. Briefly, KAF156 underwent oxygenation (M31 and M35.8), oxidative defluorination (M19), oxidative deamination (M37), combination of oxidative deamination and reduction (M37.7), hydroxylation and ring opening (M24), acetylation (M36), and hydrolytic cleavage, leading to the imidazole ring opening (M43). A combination of the above reactions and *O*-sulfonation led to the formation of several downstream less polar metabolites (M27, M28, M35, and M33) and polar metabolites (M3, M5, M7, M10, M10.1, M11, and M12).

Discussion

KAF156 is an antimalarial agent, which was designed to eradicate both blood-stage and liver-stage malaria parasites, providing a potentially new treatment of malaria prophylaxis (Kuhen et al., 2014; Diagana, 2015). To facilitate the understanding of metabolism and disposition of KAF156 in humans, ADME studies in rats and in vitro across species metabolism studies were conducted.

After intravenous or oral dosing of [^{14}C]KAF156-1, mass balance was achieved in rats. The radioactivity was excreted equally via urinary and fecal pathways. KAF156 showed high clearance, large volume of distribution and long terminal half-life in rats. After oral dosing, KAF156 was well absorbed and extensively metabolized in rats such that unchanged KAF156 accounted for only ~8–21% of the dose in feces by either dosing route. The prominent radioactive components in rat plasma were KAF156 and three oxidative metabolites (M31, M35.8,

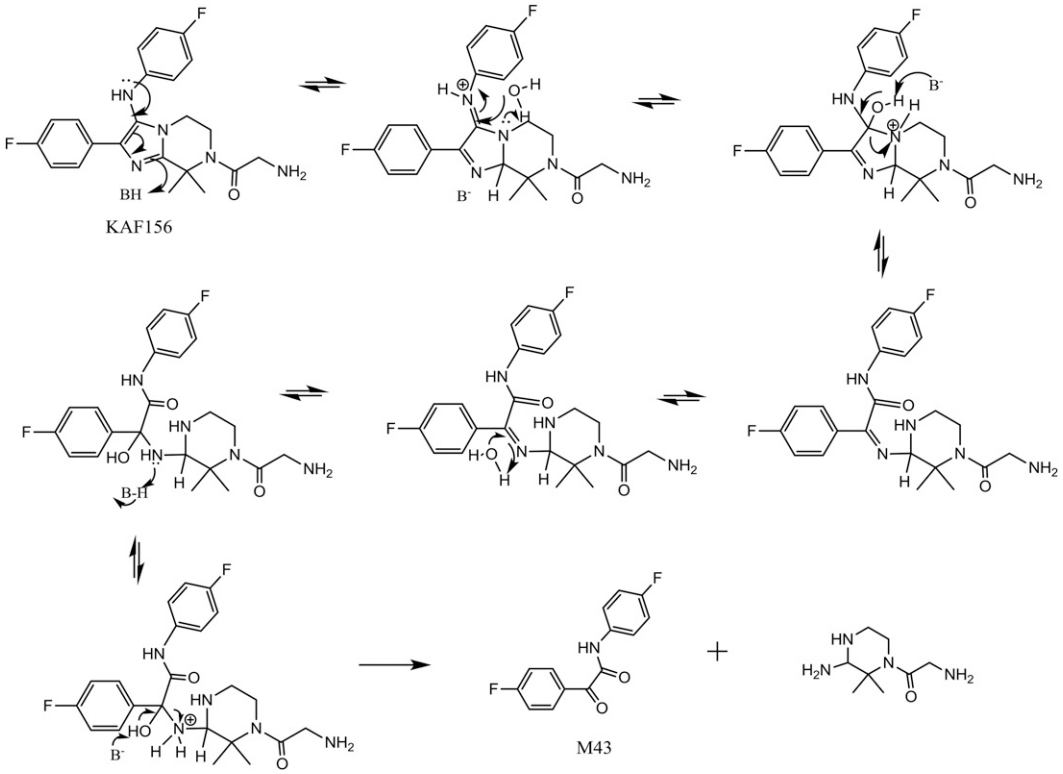

Fig. 10. Proposed mechanism for the formation of M43 from KAF156

and M37). Several metabolites were identified in urine and feces by LC-MS/MS analysis.

However, four prominent polar metabolites, accounting for ~23–35% of the dose by either dosing route were not identified in rat urine because of their low ionization efficiency under either positive or negative ion mode and the endogenous urine matrix background. To facilitate the structural characterization of polar metabolites in rat urine, we developed a new UPLC method that prolonged the retention times of these polar metabolites (Godejohann, 2007; Liu et al., 2010; Gray et al., 2011; Heaton et al., 2012). In addition, we purchased two commercially available putative metabolites (fluoroaniline and hydroxyphenylacetamide) and established their poor ionization efficiency under either positive or negative ion mode.

We decided to use the mass filter feature in the accurate mass spectrometer to accelerate the identification of polar metabolites (Ma et al., 2006; Zhang and Mitra, 2012). We designed an oral dosing solution as a mixture of [^{14}C]KAF156-1 (specific activity 3.65 μCi/mg) and [$^{13}C_6$]KAF156-1. At this stage of drug development, [$^{13}C_6$]KAF156-1 was available and used as the internal standard for the quantification of KAF156 in toxicology studies, therefore our strategy does not require extra research efforts and resources.

Theoretically, a mixture of [^{12}C]KAF156 and [$^{13}C_6$]KAF156-1 with the 0.9 mass ratio and 6.0202 mass difference would provide the same information in terms of mass filter application in accurate mass spectrometry. However, in our dual labeling approach, we strategically added trace amount of [^{14}C]KAF156-1 to allow identification of any putative metabolite that no longer satisfied either or both criteria (i.e., mass ratio or/and mass difference) of a defined mass filter. As described below, we indeed identified two metabolites (M5 and M12) that would have been missed without the addition of radiolabeled tracer in the oral dose.

As expected, three polar metabolites (M3, M10, and M11) and one less polar metabolite (M43) of KAF156 were easily identified in rat urine based on the detection of isotopic pairs of molecular ions with the expected mass ratio and mass difference. Nevertheless, M5 was not identified until the criteria of mass ratio of 0.9 was removed from the mass filter. It turned out that M5 had lost fluorine and coeluted with an endogenous substance with the identical molecular ion $[M-H]^-$ of *m/z* at 230, resulting in the change of mass response ratio of [^{12}C]/[$^{13}C_6$] from 0.9 to ~2. Interestingly, M5 was the only polar metabolite that had lost fluorine, presumably via oxidative defluorination of the fluoroaniline ring, and shared the same elemental composition as an endogenous substance. This conclusion was derived based on the detection of the endogenous substance $[M-H]^-$ of *m/z* at 230 in urine from control rats without any treatment.

Concurrently M43, an imidazole ring-opened metabolite, was identified using this dual labeling approach under negative ion mode (Supplemental Fig. S5). Apparently, M43 was derived via hydrolytic cleavage at the imidazole ring of KAF156, followed by amide hydrolysis to form a putative intermediate (fluoroaniline), which was further hydroxylated, oxidative defluorinated, acetylated, or *O*-sulfonated to generate above four polar metabolites (M3, M5, M10, and M11).

Consistent with the above in vivo findings, M43 was identified to be the major metabolite when [^{14}C]KAF156-1 was incubated with rat and human hepatocytes. However, none of polar metabolites were detected from any in vitro incubations, although most less polar metabolites identified in vivo were also generated in rat hepatocytes. The limitation of the in vitro system observed for KAF156 is not unusual, because the same experiences have been reported in the literature for many drug candidates. Therefore, the characterization of polar metabolites of KAF156 could only be achieved from an in vivo study.

Accordingly, we were concerned that we may miss the identification of putative metabolites derived from hydrolysis of M43, which may have lost the radiolabeling of [^{14}C]KAF156-1 and stable isotope labeling of [$^{13}C_6$]KAF156-1 (e.g., metabolites containing fluorophenyl ring). It

would be challenging to identify these putative polar metabolites under either positive or negative ion mode without any mass filter.

Subsequently, we initiated synthesis of another tracer ([^{14}C]KAF156-2) and strategically radiolabeled the carbon in the imidazole ring adjacent to fluorophenyl ring to allow detection of any putative hydrolysis metabolites of M43. After intravenous or oral dosing of [^{14}C]KAF156-2, mass balance was achieved in rats. However, another three polar metabolites in rat urine, accounting for ~13–14% of the dose by either dosing route, were detected but could not characterized by LC-MS/MS analysis due to low ionization efficiency.

To enable the identification of polar metabolites using the same dual labeling approach, we considered two strategies for the stable isotope labeling of KAF156: (A) [$^{13}C_6$]KAF156-3 with stable isotope labeling at six carbon atoms of the fluorophenyl ring and (B) [$^{13}C_2$]KAF156-2 with the stable isotope labeling at two adjacent carbon atoms of the imidazole portion of KAF156 (Fig. 1). Based on the fact that carbon atom adjacent to fluorophenyl ring was radiolabeled in [^{14}C]KAF156-2, we anticipated [$^{13}C_2$]KAF156-2 and [^{14}C]KAF156-2 together would provide us with more information regarding any putative metabolism occurring at imidazolopiperazine moiety. We designed the oral dose as a mixture of [^{14}C]KAF156-2 (specific activity 3.1 μCi/mg) and [$^{13}C_2$]KAF156-2 with the mass ratio of [^{12}C]/[$^{13}C_2$] of 0.9 and the mass difference of 2.006.

As expected, two polar metabolites (M7 and M10.1) containing fluorophenyl ring were identified in rat urine using a defined mass filter. However, M12 was detected by radioactivity but was not selected using the above isotopic mass ratio and mass difference as mass filters. Apparently, M12 lost one labeled carbon atom during biotransformation and could no longer be detected using the above mass filters. Therefore, we initiated the isolation of these polar metabolites from rat urine and elucidated the structure of M12 by NMR and LC-MS/MS analyses. M12 was assigned as a glycine conjugate of fluorobenzoic acid, presumably M7 underwent oxidative decarboxylation and followed by glycine conjugation. Retrospectively, M12 could have been easily identified by LC-MS/MS analysis using the dual labeling approach (strategy A). We did not identify any other new metabolites containing portion of imidazolopiperazine using strategy B.

The formation of imidazole ring opened metabolite M43 was further investigated. As mentioned previously, M43 was identified to be the major metabolite when [^{14}C]KAF156-1 was incubated with rat and human hepatocytes. In addition, M43 was detected at low level when incubated in buffer without hepatocytes (pH 7.4) for 24 hours. These findings suggest that the hydrolytic cleavage of imidazole ring was catalyzed enzymatically and with some extent of chemical degradation during hepatocyte incubations. However, M43 was not generated when [^{14}C]KAF156-1 was incubated with all 19 commercially available recombinant CYP enzymes in the presence of NADPH, indicating that this is not CYP450 catalyzed reaction (data not shown). Therefore, a two-step hydrolytic cleavage mechanism for the formation of M43 from KAF156 is proposed (Fig. 10).

Overall, the dual labeling approach proved to be practical and valuable in the elucidation of polar metabolites of KAF156 with low molecular weights and low ionization efficiency by either positive or negative mode. This approach has been shown to be superior to using stable isotope labeling alone in cases where unexpected biotransformations occurred. However, the decisions regarding the positions of stable isotope labeling and radiolabeling require careful consideration and biotransformation insight.

Acknowledgments

The authors thank Dr. Francis Tse for constructive discussions and continued encouragement and support, Professor Phil Huskey (Rutgers University) for constructive discussion of reaction mechanism, Dr. Amy Wu and Mr. Lawrence Jones for the purification and analytical certification of [^{14}C]KAF156, and Dr. Tapan Majumdar and Ms. Shari Wu for the quantification of KAF156 in rat plasma.

Authorship Contributions

Participated in study design: Huskey, Jian, Ray, He, and Flarakos.
Conducted experiments: Forseth, Li, and Zhang.
Performed chemical synthesis: Forseth and Jian.
Performed data analysis: Huskey, Forseth, Li, Catoire, and Zhang.
Wrote or contributed to the writing of manuscript: Huskey, Forseth, and Mangold.

References

Amet S, Zimner-Rapuch S, Launay-Vacher V, Janus N, and Deray G (2013) Malaria prophylaxis in patients with renal impairment: a review. *Drug Saf* **36**:83–91.
Carter TE, Boulter A, Existe A, Romain JR, St Victor JY, Mulligan CJ, and Okech BA (2015) Artemisinin resistance-associated polymorphisms at the K13-propeller locus are absent in Plasmodium falciparum isolates from Haiti. *Am J Trop Med Hyg* **92**:552–554.
Chavez F, Kennedy N, Rawalpally T, Williamson RT, and Cleary T (2010) Substituents effect on the Erlenmeyer-Plöchl reaction: Understanding an observed process reaction time. *Org Process Res Dev* **14**:579–584.
Diagana TT (2015) Supporting malaria elimination with 21st century antimalarial agent drug discovery. *Drug Discov Today* **20**:1265–1270.
Godejohann M (2007) Hydrophilic interaction chromatography coupled to nuclear magnetic resonance spectroscopy and mass spectroscopy–a new approach for the separation and identification of extremely polar analytes in bodyfluids. *J Chromatogr A* **1156**:87–93.
Gray N, Musenga A, Cowan DA, Plumb R, and Smith NW (2011) A simple high pH liquid chromatography-tandem mass spectrometry method for basic compounds: application to ephedrines in doping control analysis. *J Chromatogr A* **1218**:2098–2105.
Haque U, Glass GE, Haque W, Islam N, Roy S, Karim J, and Noedl H (2013) Antimalarial drug resistance in Bangladesh, 1996-2012. *Trans R Soc Trop Med Hyg* **107**:745–752.
Heaton J, Gray N, Cowan DA, Plumb RS, Legido-Quigley C, and Smith NW (2012) Comparison of reversed-phase and hydrophilic interaction liquid chromatography for the separation of ephedrines. *J Chromatogr A* **1228**:329–337.
Held J, Jeyaraj S, and Kreidenweiss A (2015) Antimalarial compounds in Phase II clinical development. *Expert Opin Investig Drugs* **24**:363–382.
Hott A, Casandra D, Sparks KN, Morton LC, Castanares G-G, Rutter A, and Kyle DE (2015) Artemisinin-resistant Plasmodium falciparum parasites exhibit altered patterns of development in infected erythrocytes. *Antimicrob Agents Chemother* **59**:3156–3167.
Kuhen KL, Chatterjee AK, Rottmann M, Gagaring K, Borboa R, Buenviaje J, Chen Z, Francek C, Wu T, Nagle A, et al. (2014) KAF156 is an antimalarial clinical candidate with potential for use in prophylaxis, treatment, and prevention of disease transmission. *Antimicrob Agents Chemother* **58**:5060–5067.
Lee DG and Chen T (1991) The oxidation of alcohols by permanganate. A comparison with other high-valent transition-metal oxidants. *J Org Chem* **56**:5341–5345.
Leong FJ, Zhao R, Zeng S, Magnusson B, Diagana TT, and Pertel P (2014) A first-in-human randomized, double-blind, placebo-controlled, single- and multiple-ascending oral dose study of novel Imidazolopiperazine KAF156 to assess its safety, tolerability, and pharmacokinetics in healthy adult volunteers. *Antimicrob Agents Chemother* **58**:6437–6443.
Liu M, Ronk M, Ren D, Ostovic J, Cauchon N, Zhou ZS, and Cheetham J (2010) Structure elucidation of highly polar basic degradants by on-line hydrogen/deuterium exchange hydrophilic interaction chromatography coupled to tandem mass spectrometry. *J Chromatogr A* **1217**:3598–3611.
Ma S, Chowdhury SK, and Alton KB (2006) Application of mass spectrometry for metabolite identification. *Curr Drug Metab* **7**:503–523.
Meister S, Plouffe DM, Kuhen KL, Bonamy GM, Wu T, Barnes SW, Bopp SE, Borboa R, Bright AT, Che J, et al. (2011) Imaging of Plasmodium liver stages to drive next-generation antimalarial drug discovery. *Science* **334**:1372–1377.
Nagle A, Wu T, Kuhen K, Gagaring K, Borboa R, Francek C, Chen Z, Plouffe D, Lin X, Caldwell C, et al. (2012) Imidazolopiperazines: lead optimization of the second-generation antimalarial agents. *J Med Chem* **55**:4244–4273.
Na-Bangchang K and Karbwang J (2013) Emerging artemisinin resistance in the border areas of Thailand. *Expert Rev Clin Pharmacol* **6**:307–322.
Nahrendorf W, Scholzen A, Sauerwein RW, and Langhorne J (2015) Cross-stage immunity for malaria vaccine development. *Vaccine* **33**:7513–7517.
Sagara I, Oduro AR, Mulenga M, Dieng Y, Ogutu B, Tiono AB, Mugyenyi P, Sie A, Wasunna M, Kain KC, et al. (2014) Efficacy and safety of a combination of azithromycin and chloroquine for the treatment of uncomplicated Plasmodium falciparum malaria in two multi-country randomised clinical trials in African adults. *Malaria J* **13**:458–467.
Teneza-Mora N, Lumsden J, and Villasante E (2015) A malaria vaccine for travelers and military personnel: Requirements and top candidates. *Vaccine* **33**:7551–7558.
Witkowski B, Khim N, Chim P, Kim S, Ke S, Kloeung N, Chy S, Duong S, Leang R, Ringwald P, et al. (2013) Reduced artemisinin susceptibility of Plasmodium falciparum ring stages in western Cambodia. *Antimicrob Agents Chemother* **57**:914–923.
Wu T, Nagle A, Kuhen K, Gagaring K, Borboa R, Francek C, Chen Z, Plouffe D, Goh A, Lakshminarayana SB, et al. (2011) Imidazolopiperazines: hit to lead optimization of new antimalarial agents. *J Med Chem* **54**:5116–5130.
Zhang Z and Mitra K (2012) Application of mass spectrometry for metabolite identification, in *ADME-Enabling Technologies in Drug Design and Development* (Zhang D and Surapaneni S eds) pp 317–330, John Wiley & Sons, Inc., Hoboken, NJ.

Address correspondence to: Su-Er Wu Huskey, Novartis Institutes for BioMedical Research, One Health Plaza, East Hanover, NJ 07936-1080. E-mail: Su.huskey@novartis.com